Image-Charge Effects in Electron-Stimulated Desorption: O^- from O_2 Condensed on Ar Films Grown on Pt

H. Sambe and D. E. Ramaker
Chemistry Department, George Washington University, Washington, D.C. 20052

and

L. Parenteau and L. Sanche
Canadian Medical Research Council Group in Radiation Sciences, Faculty of Medicine, University of Sherbrooke, Sherbrooke, Quebec J1H 5N4, Canada
(Received 2 March 1987)

The electron-stimulated desorption yields of O^- from O_2 condensed on a platinum substrate, with a rare-gas spacer layer between the O_2 and Pt, are reported. The results differ dramatically from those found in the gas phase. These differences are interpreted in terms of the image charge induced in the metal.

PACS numbers: 79.20.Kz, 31.70.Ks, 34.80.Gs, 82.65.Nz

The interaction of an ion with a metal surface is dominated by the image charge induced in the metal substrate.[1] The role that the image-charge force plays in ion scattering or desorption from a metal surface has been studied theoretically,[2-4] but no clear-cut experimental data have been presented. This arises in part because of the difficulty in isolating the image-charge effects from other effects, such as ion neutralization and multiple scattering.

In this Letter we present electron-stimulated desorption (ESD) yields of O^- from O_2 condensed on polycrystalline Pt in the electron-energy range 0–40 eV. The effects of ion neutralization are minimized by inserting a rare-gas (Ar, Kr, or Xe) layer between the Pt metal and the O_2 layer. The rare-gas layer also serves as a spacer layer so that the distance between the ion and the metal surface can be varied, thus varying the effect of the image-charge force on the desorbing ions.[5] Moreover, there are two advantages of the current O_2/rare-gas/Pt system over the previously studied O_2/Pt system.[6] First, features due to multiple-electron-scattering processes are more easily identifiable. Second, the interaction between an O_2 molecule and neighboring rare-gas atoms in the present system is much weaker than the interaction between neighboring O_2 molecules in the earlier system. The weaker interaction reduces the effect of intermolecular deexcitation or neutralization. These advantages make it easier to isolate the image-charge effects, which are seen to have a dramatic effect on the desorption yield.

The electron-impact O^- dissociation of O_2 gas is well understood.[7] The electron-energy dependence of the O^- yield is shown in Fig. 1 (top curve from Rapp and Briglia[8]). In the energy range from 4.4 to 10 eV, the O^- ions are produced via the transient $O_2^-(^2\Pi_u)$ anion. This process,

$$e^- + O_2(^3\Sigma_g^-) \rightarrow O_2^-(^2\Pi_u) \rightarrow O^-(^2P) + O(^3P),$$

is referred to as dissociative attachment (DA). Above 17 eV, the O^- ions are produced predominantly via an excited neutral O_2^* molecule. This process,

$$e^- + O_2(^3\Sigma_g^-) \rightarrow O_2^* \rightarrow O^- + O^+,$$

is referred as dipolar dissociation (DD).

The apparatus has been previously described.[9] A rare gas is condensed near its sublimation temperature on a clean Pt ribbon, and the O_2 gas is condensed onto the rare-gas film at 17 K. The film thicknesses are estimated to within 20% by a method described previously.[10] The incidence angle of the electron beam is 20° from the surface, and the O^- ions are measured by a quadrupole mass spectrometer positioned at 70° from the surface.

Figure 1 compares the electron-energy dependence of the ESD O^- yield from O_2 gas with that from the O_2/Ar/Pt samples, where the O_2 coverage is kept constant at 0.1 ML (monolayer) and the Ar thickness is varied from 0.37 to 4.3 ML. As the Ar thickness increases, the four features indicated by arrows at around 6, 14, 18, and 24 eV grow faster than the remainder of the spectrum and at large thicknesses (i.e., > 20 ML) dominate the spectrum. These four features contain contributions from multiple electron scattering which involve energy-loss processes in Ar or O_2. Details of these assignments will be published elsewhere.[11] What is significant here is that the contributions from multiple electron scattering are relatively small below 2.2 ML, so that the O^- yields at 6 eV and above 17 eV can be considered to arise mainly from the DA and DD processes, respectively, as in gaseous O_2. The replacement of Ar by Kr or Xe in O_2/Ar/Pt gives similar results.

Figure 2 shows the Ar-thickness dependence of the O^- yield from O_2/Ar/Pt with a constant (0.1 ML) O_2 coverage. At 30 and 40 eV, we expect only small multiple-electron-scattering contributions for the range of Ar thicknesses given in Fig. 2. Although multiple

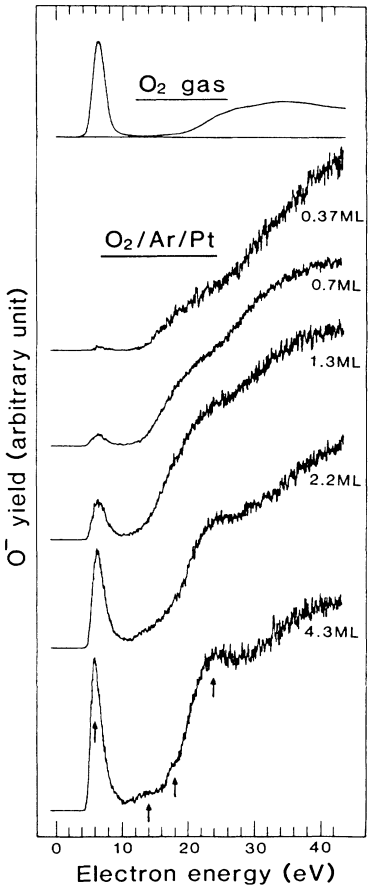

FIG. 1. Comparison of O^- yield curves produced by ESD from O_2 gas (Ref. 8) with those from O_2/Ar/Pt samples with a constant (0.1 ML) O_2 coverage and variable (0.37–4.3 ML) Ar thicknesses. Arrows indicate features involving multiple electron scattering.

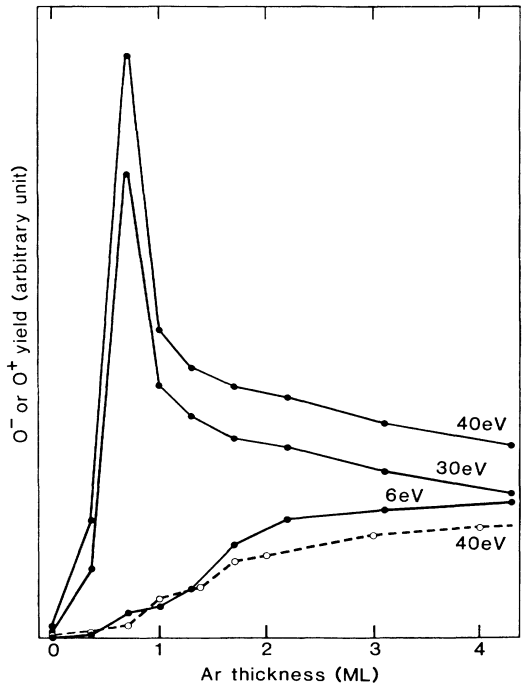

FIG. 2. Ar-thickness dependence of the O^- yields produced by ESD from the O_2/Ar/Pt samples with a constant (0.1 ML) O_2 coverage. The incident electron energies are as indicated. Also shown (dashed curve) is the O^+ yield produced by ESD with incident energy of 40 eV on O_2(0.16 ML)/Ar (variable)/Pt.

electron scattering contributes above 2.2 ML Ar, this contribution in no way alters the conclusions that the O^- yield via the DA process increases with Ar thickness, while the O^- yield via the DD process decreases with Ar thickness beyond 0.7 ML Ar. Within the accuracy of our Ar-thickness measurements, we may state that the sharp maximum probably corresponds to the case when the Ar plus O_2 coverage form 1 ML. Replacement of Ar by Kr or Xe in O_2/Ar/Pt gives similar results.

Figure 2 also shows the O^+ yield from O_2(0.16 ML)/Ar(variable)/Pt samples produced by 40-eV electron impact. In O_2 gas, O^+ formation by 40-eV electron impact arises predominantly via an O_2^+ intermediate state.[12] Therefore, we expect that both the O^+ yield and the DA contribution to the O^- yield are produced via charged intermediate states, O_2^+ and O_2^-, respectively. Figure 2 shows that the image charge has a similar effect on these charged states and their dissociated ions.

The image charge induced in the Pt metal plays a central role in our explanation for the experimental results described above. Table I summarizes four effects that the image charge has on the desorption yield. We explain the first three effects using the semiquantitative, adiabatic potential-energy curves for O_2 as depicted in Fig. 3. The solid curves give the ground state of O_2, the $^2\Pi_u$ O_2^- state and its partner dissociating to the lowest $O^- + O$ limit, and an O_2^* state and its partner dissociating to the lowest $O^+ + O^-$ limit.[13] The two O_2^- and two O_2^* states each form a pair of states which at large separation have wave functions approaching $[\psi(O_a^-)\times\psi(O_b)\pm\psi(O_a)\psi(O_b^-)]$ and $[\psi(O_a^+)\psi(O_b^-)\pm\psi(O_a^-)\psi(O_b^+)]$, respectively, where $\psi(O_a)$ denotes the wave function for an isolated O atom at site a. The dotted curves give the corresponding potential-energy curves in the presence of the image charge. The symbol O^+/M in Fig. 3, for example, means that the O^+ ion is near a metal surface. The image charge due to the Pt lowers the energies of the ionic species such as O^+/M, O^-/M, and O_2^-/M, while the energies of the neutral species such as O/M, O_2^*/M, and O_2/M remain the same. The magnitude of this lowering depends on the distance between the ion and the metal surface, and hence on the thickness of the rare-gas spacer layer. The

TABLE I. Summary of image-charge effects on the O^- yield via the dissociative-attachment (DA) and dipolar-dissociation (DD) processes. The effect indicated for each contribution (increase, decrease, or no change) is relative to the O^- yield from O_2 gas. The relative magnitude of the effect [large (L) or small (S)] for a given image-charge strength is indicated in parentheses.

Image-charge effect	DA contribution	DD contribution
Dissociation branching	Decrease(L)	Increase(S)
O^- kinetic energy	Decrease(S)	Increase(S)
Configuration space	Decrease(S)	Increase(L)
Intermediate-state quenching[a]	Decrease(L)	No change[b]

[a]Active only when the O_2 intermediate has significant orbital overlap with the metal surface.

[b]Although intermediate-state quenching causes a reduction in the DD contribution for O_2/Ar/Pt relative to O_2 gas, the magnitude of this effect is not changed by the image charge.

curves in Fig. 3 are schematically drawn with the maximum energy lowering, 2.5 eV.[14]

The first effect of the image charge involves the energy separation of the $O+O^-$ dissociation limit into the $O/M+O^-$ and $O^-/M+O$ limits. Consequently, to desorb O^- ions, the lower $O_2{}^-/M$ intermediate state must undergo a nonradiative transition into its upper partner state. The mechanism for this "charge transfer" transition, $O^-/M+O$ to $O/M+O^-$, is similar to that for symmetric charge transfer in atom-atom collisions of identical nuclei[15] and occurs because of the breakdown of the adiabatic approximation. The probability for this transition is $\frac{1}{2}$ when the separation of the dissociation limits vanishes, and decreases quickly as the separation increases. In contrast, the separation between the $O^-/M+O^+$ and O^-+O^+/M dissociation limits is negligibly small. Nevertheless, on the basis of the relative atomic sizes of O^+ and O^-, we expect that the O^-+O^+/M limit is slightly lower than the $O^-/M+O^+$ limit. This means that the DA contribution should increase and the DD contribution should decrease slightly as the thickness of the rare-gas layer increases.

The second effect of the image charge involves the kinetic energy of the escaping O^- ions. As can be seen easily in Fig. 3, in comparison with the corresponding O^- kinetic energy from O_2 gas, the kinetic energy of the O^- ions via $O_2{}^-/M$ is decreased while that via $O_2{}^*/M$ is increased. The slower-escaping ions have a greater chance to be recaptured or neutralized, thus decreasing the DA O^- yield, while the faster O^- ions have a greater chance for escape, thus increasing the DD O^- yield. We expect, however, that this mechanism causes a relatively small effect.

The third effect of the image charge involves the number of vibrational and/or electronic intermediate states

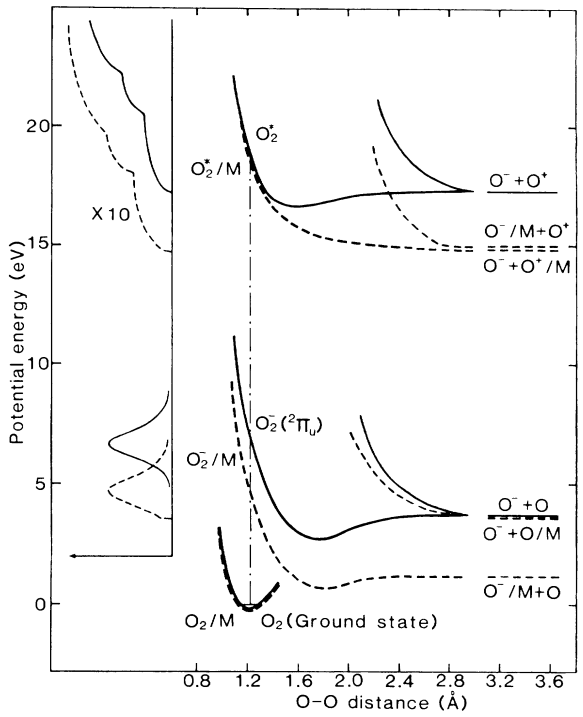

FIG. 3. Potential-energy curves of O_2 gas (solid curves) and the corresponding potential-energy curves under the influence of an image charge (dashed curves). Spectra on the left side show schematically the relative number of vibrational and/or electronic states which have sufficient energy to yield O^- ions, for O_2 gas (solid lines) and for O_2/M (dashed lines).

(i.e., amount of configuration space) which have sufficient energy to yield O^- ions. The curves on the left-hand side of Fig. 3 schematically indicate the configuration space for production of O^- from O_2 gas (solid lines) and from O_2/M (dashed lines). These plots indicate that the configuration space for $O_2{}^-/M$ decreases slightly while that for the $O_2{}^*/M$ state increases significantly compared with that for O_2.

Finally, the fourth effect of the image charge involves the quenching rate of the intermediate state. Near a metal surface, some of the $O_2{}^-$ or $O_2{}^*$ states may be neutralized or deexcited before the desorption process can get underway. The image charge influences these destruction rates of the $O_2{}^-$ intermediate state by attracting the ion towards the metal surface. The inward motion and subsequent neutralization are similar to the first two steps of the Antoniewicz "bounce" mechanism,[16] which is known to be active for neutral desorption from physisorbed systems.[17] Again, in contrast, the deexcitation rate of the $O_2{}^*$ intermediate state is not affected by the image charge. Thus, intermediate-state quenching has a greater effect on the DA process than on the DD process.

As summarized in Table I, all four image-charge

mechanisms predict a depletion of the DA process relative to the DD process. This is consistent with the two-orders-of-magnitude reduction in the O^-(via DA)/O^-(via DD) ratio for the O_2(0.37 ML)/Ar/Pt system compared with that of the O_2 gas in Fig. 1. As the thickness of the rare-gas spacer layer decreases from 4 to 1 ML, the image-charge force increases. Accordingly, with decreasing rare-gas thickness, the O^- yield via the DA process should decrease and that via the DD process should increase. This is consistent with Fig. 2. As indicated above and summarized in Table I, the dissociation branching effect for the DA process, and the configuration-space effect for the DD process, are primarily responsible for this behavior.

The increase in O^- yield with increasing Ar coverage below 0.7 ML (Fig. 2) does not arise from any of the four image-charge mechanisms in Table I because the image-charge force is constant until the O_2 plus Ar form 1 ML. We believe the O^- yield increases because the Ar atoms (1) interfere with the metallic neutralization of the escaping O^- ions and (2) encourage orientation of the O_2 molecules normal to the metal surface.

The work two of the authors (H.S. and D.E.R.) was supported in part by the U. S. Office of Naval Research.

[1]H. Margenau and N. R. Kestner, *Theory of Intermolecular Forces* (Pergamon, New York, 1971), 2nd ed., p. 329.

[2]J. W. Gadzuk and J. K. Norskov, J. Chem. Phys. **81**, 2828 (1984); J. W. Gadzuk and S. Holloway, Phys. Scr. **32**, 413 (1985).

[3]W. L. Clinton, Surf. Sci. **112**, 791 (1981).

[4]Z. Miskovic, J. Vukanic, and T. E. Madey, Surf. Sci. **141**, 285 (1984).

[5]T. C. Chiang, G. Kaindl, and D. E. Eastman, Solid State Commun. **41**, 661 (1982), and **36**, 25 (1980), and Phys. Rev. Lett. **45**, 1808 (1980).

[6]L. Sanche, Phys. Rev. Lett. **53**, 1638 (1984).

[7]G. J. Schulz, Rev. Mod. Phys. **45**, 423 (1973); R. Locht and J. Momigny, Int. J. Mass Spectrom. Ion Phys. **7**, 121 (1971).

[8]D. Rapp and D. D. Briglia, J. Chem. Phys. **43**, 1480 (1965).

[9]L. Sanche and L. Parenteau, J. Vac. Sci. Technol. A **4**, 1240 (1986).

[10]L. Sanche, J. Chem. Phys. **71**, 4860 (1979); E. Keszei *et al.*, J. Chem. Phys. **85**, 7396 (1986).

[11]H. Sambe *et al.*, to be published.

[12]R. Locht and J. Schopman, Int. J. Mass Spectrom. Ion Phys. **15**, 361 (1974), and Chem. Phys. Lett. **26**, 596 (1974).

[13]F. R. Gilmore, J. Quant. Spectrosc. Radiat. Transfer **5**, 369 (1965).

[14]Estimated for O_2/Pt with the measured value (2.14 eV) for Xe/Pd reported in Ref. 5.

[15]S. Geltman, *Topics in Atomic Collision Theory* (Academic, New York, 1969).

[16]P. R. Antoniewicz, Phys. Rev. B **21**, 3811 (1980).

[17]P. Feulner *et al.*, Phys. Rev. Lett. **53**, 671 (1984); Q. J. Zhang, R. Gomer, and D. R. Bowman, Surf. Sci. **129**, 535 (1983).